Supplementary Information

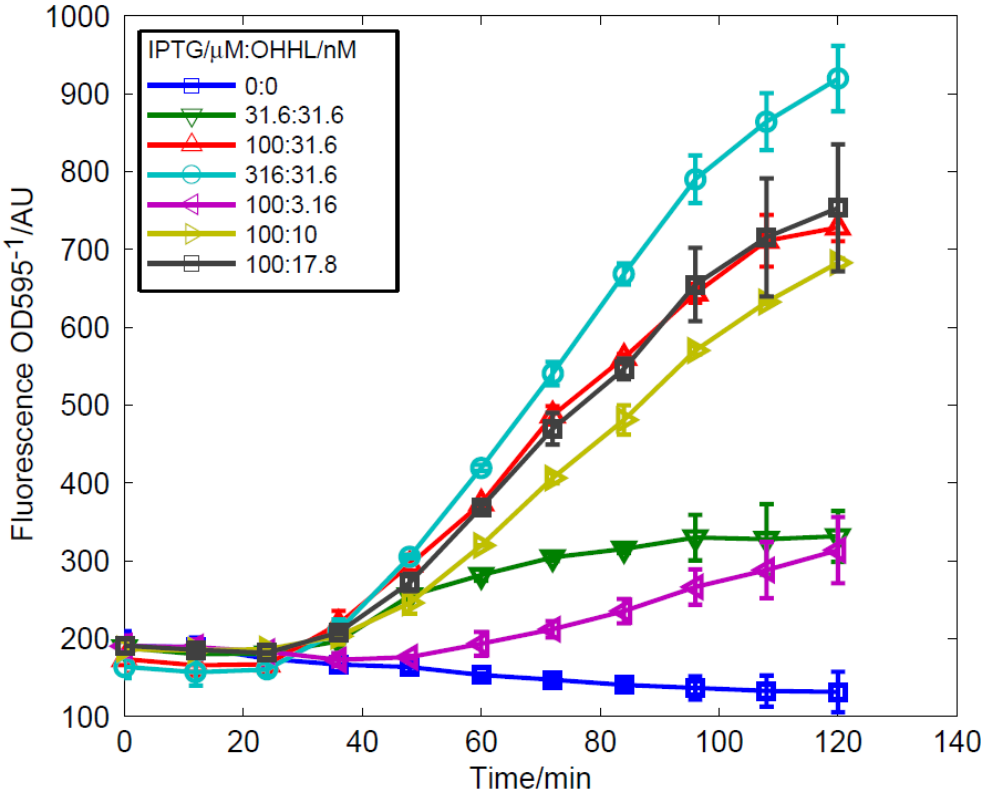

Figure S1. Population level responses of coupled positive-negative feedback loop circuit. Responses were measured using a Gemini XPS microplate spectrofluorometer with samples maintained at 37°C with shaking between measurements. Error bars are standard deviations from 3 independent cultures.

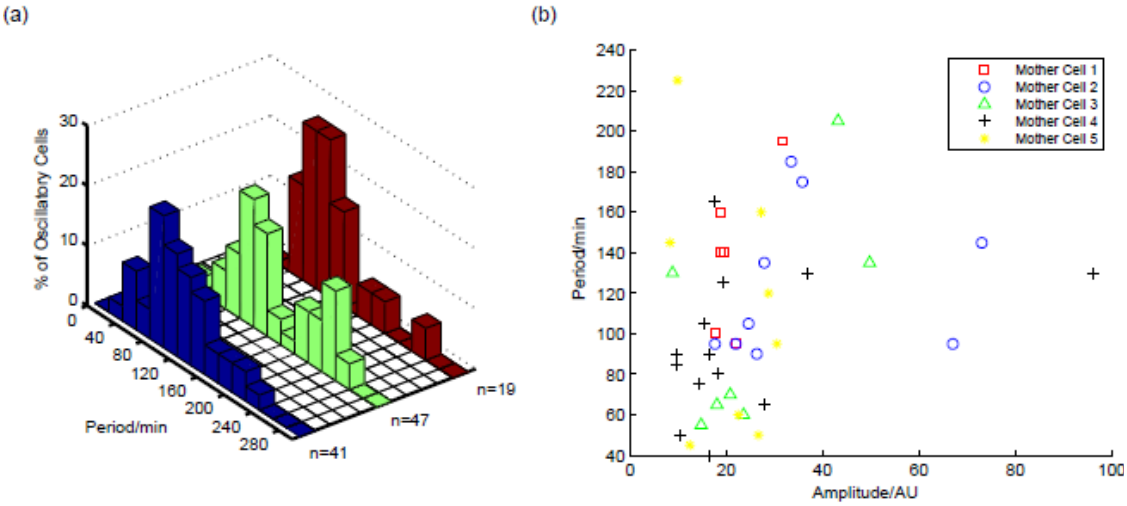

Figure S2. Variation in the responses of the coupled feedback loop circuit. (a) Histograms of measured periods for default coupled feedback loop circuit measured on different days. (b) Dependence of period on peak amplitude for multiple mother cells measured on the same day. Note the wide variation in both the amplitudes and periods measured for individual mother cells and the lack of any discernable correlation between the two properties.

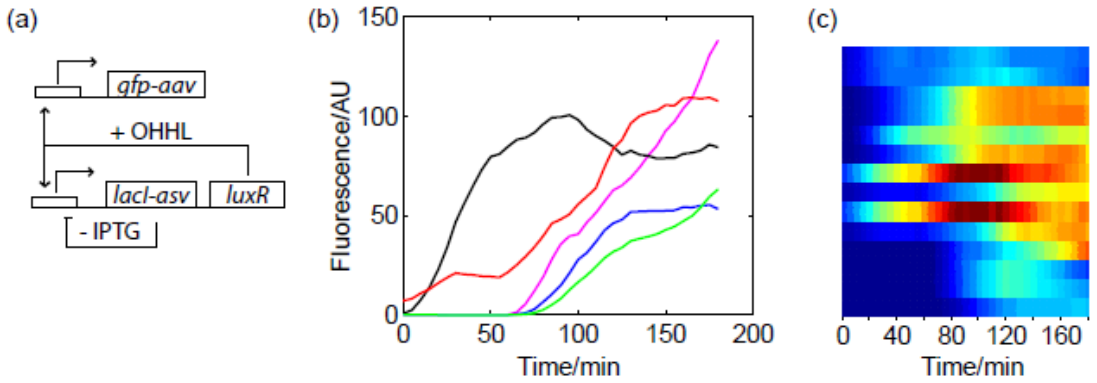

Figure S3. Examination of LuxR degradation during circuit expression. (a) Design of control circuit. GFPmut2-aav expression from P_{luxI} measures LuxR activity independent of LacI repression. (b) Fluorescence trajectories for control cells. None of the trajectories show a rapid fluorescence loss that would indicate rapid degradation of the LuxR protein during LacI repression of $P_{luxI\text{-}lacO(14TC)}$. (c) Additional heat map trajectories of cells containing the control circuits.

Table S1. Primers used for construction of coupled feedback loop circuit and controls. Sequences that hybridize to the target sequence are underlined, and ssrA tags are italicized. Restriction digests sites are given as lower case letters.

Primer	Sequence
LuxR – F: NheI	ATA gctagc ATG AAA AAC ATA AAT GC
LuxR – R: KpnI	ATC ggtacc TTA ATT TTT AAA GTA TGG GCA ATC
LacI – F: KpnI	TA ggtacc GGA AGA GAG TCA ATT CAG GG
LacI(asv*)* – R: EcoRI	TT gaattc *TTA AAC TGA TGC AGC GTA GTT TTC GTC GTT TGC TGC* CTG CCC GCT TTC CAG TC
GFP – F: EcoRI	TA gaattc AGG GAG GTT GGT ATG AGT AAA GGA GAA GAA C
GFP(aav*)* – R: PvuI	AT cgatcg *TTA AAC TGC TGC AGC GTA GTT TTC GTC GTT TGC TGC* TTT GTA GAG CTC ATC C
GroE – F: EcoRI	G gaattc GTC ACC CAT AAC AGA TAC GG
GroE – R: AvrII	T cctagg TTA CAT CAT GCC GCC CAT GC
P_{luxI} – F: PciI	acatgt AGT CCT TTG ATT CTA ATA AAT TGG ATT TTT
$P_{luxI\text{-}lacO}$ – F: AatII	gacgtc AGT CCT TTG ATT CTA ATA AAT TGG ATT TTT
$P_{luxI\text{-}lacO}$ – R (14TC): NheI	ATA gctagc ACC AAC CTC CCT TTA AGC TTG GAA TTG TTG TCC GCT CAC
P_{bla} –F: PciI	TAT acatgt CAG GTG GCA CTT TTC G

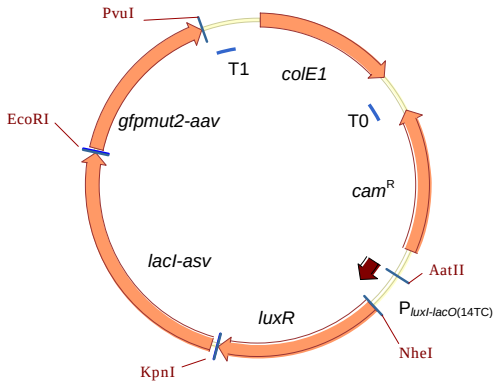

p*luxI-lacO*(14TC)_R**I***asv***G***aav*

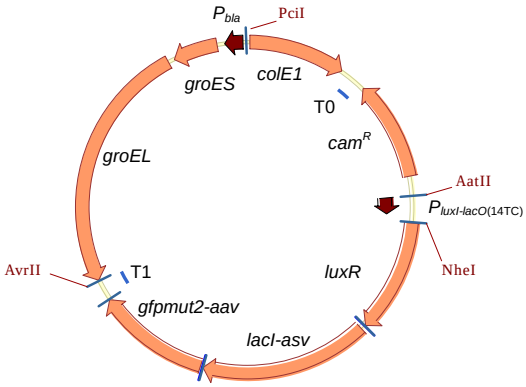

p*luxI-lacO*(14TC)_R**I***asv***G***aav_bla*_GroE

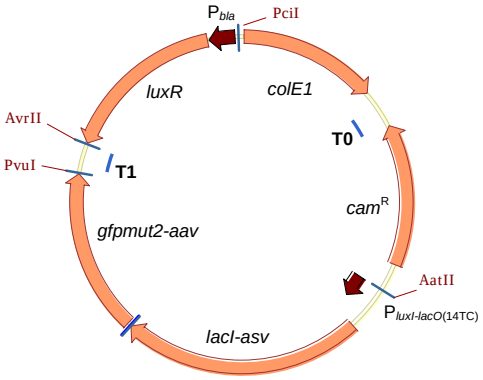

p*luxI-lacO*(14TC)_**I***asv***G***aav_bla*_R

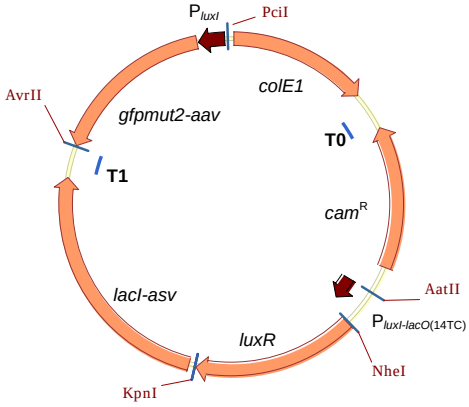

p*luxI-lacO*(14TC)_R**I***asv***_*luxI*_G*aav*

Figure S4. Plasmid maps for coupled feedback loop circuit and controls.

Modeling

We used a simple mathematical model prior to constructing our circuit to identify the interactions that have the greatest influence on the behavior of our design. The full model consists of a network of 11 coupled differential equations that describe the reactions given in Table S2. The equations are given below:

Promoter Dynamics

$$\frac{dP_{IO}}{dt} = k_{-AP}P_{IO}^{A} + k_{-IP}P_{IO}^{I} + k_{dR}P_{IO}^{A} + k_{dI}P_{IO}^{I} - k_{AP}P_{IO}A_2 - k_{IP}P_{IO}I_4$$

$$\frac{dP_{IO}^{A}}{dt} = k_{AP}P_{IO}A_2 - k_{-AP}P_{IO}^{A} - k_{dR}P_{IO}^{A}$$

$$\frac{dP_{IO}^{I}}{dt} = k_{IP}P_{IO}I_4 - k_{-IP}P_{IO}^{I} - k_{dI}P_{IO}^{I}$$

LuxR, LacI, and GFP balances

$$\frac{dR}{dt} = k_{tR}M + k_{-A}A - k_A(R)(OHHL) - k_{dR}R$$

$$\frac{dA}{dt} = k_A(R)(OHHL) + 2k_{-2A}A_2 - k_{-A}A - 2k_{2A}A^2 - k_{dR}R$$

$$\frac{dA_2}{dt} = k_{2A}A^2 + k_{-AP}P_{IO}^{A} - k_{-2A}A_2 - k_{AP}P_{IO}A_2 - k_{dR}R$$

$$\frac{dI}{dt} = k_{tI}M + 2k_{-2I}I_2 - 2k_{2I}I^2 - k_{dI}I$$

$$\frac{dI_2}{dt} = k_{2I}I_2 + 2k_{-4I}I_4 - 2k_{4I}I_2^2 - k_{dI}I$$

$$\frac{dI_4}{dt} = k_{4I}I_2^2 + k_{-IP}P_{IO}^{I} - k_{IP}P_{IO}I_4 - k_{-4I}I_4 - k_{dI}I$$

$$\frac{dG}{dt} = k_{tG}M - k_{dG}G$$

mRNA

$$\frac{dM}{dt} = k_{tm}P_{IO} + k_{tmA}P_{IO}^{A} - k_{dM}M$$

Table S2. Reactions described by model.

Reaction	Description
$P_{IO} + A_2 \underset{k-AP}{\overset{kAP}{\Leftrightarrow}} P_{IO}^{A}$	Promoter binding by activator complex
$P_{IO} + I_4 \underset{k-IP}{\overset{kIP}{\Leftrightarrow}} P_{IO}^{I}$	Promoter binding by LacI
$P_{IO} \overset{ktm}{\Rightarrow} P_{IO} + M$	Basal transcription of polycistronic mRNA
$P_{IO}^{A} \overset{ktmA}{\Rightarrow} P_{IO}^{A} + M$	Activated transcription
$M \overset{ktR,I,G}{\Rightarrow} M + R, I, G$	Translation of LuxR, LacI, GFP
$I + I \underset{k-2I}{\overset{k2I}{\Leftrightarrow}} I_2$	Dimerization of LacI
$I + I \underset{k-4I}{\overset{k4I}{\Leftrightarrow}} I_4$	Tetramerization of LacI
$R + OHHL \underset{k-A}{\overset{kA}{\Leftrightarrow}} A$	Activation of LuxR by OHHL
$A + A \underset{k-2A}{\overset{k2A}{\Leftrightarrow}} A_2$	Dimerization of activator complex
$M \overset{kdM}{\Rightarrow}$	Degradation of mRNA
$R, A, A_2, P_{IO}^{A} \overset{kdR}{\Rightarrow}$	Degradation of LuxR and LuxR complexes
$I, I_2, I_4, P_{IO}^{I} \overset{kdI}{\Rightarrow}$	Degradation of LacI and LacI complexes

In addition to these equations, we also assume that the binding rate of LacI to $P_{luxI\text{-}lacO}$ (k_{IP}) is negatively affected by IPTG according to a hill function:

$$k_{IP} = \frac{k_{IP\max}}{1 + \left(\frac{IPTG}{K_{ID}}\right)^{n}}$$

where n=2.

In order for the model to be able to predict the responses of the coupled feedback loops, appropriate values for the parameters first had to be obtained. We based the initial values of the model parameters on values given in the literature. In particular, extensive data exists for the molecular interactions of the LacI protein[1, 2], and to a lesser degree, the LuxR protein[3, 4]. mRNA and protein degradation rates are also fairly well bounded in *E. coli* with mRNAs having half-lives that are on the order of a few minutes[5], and proteins having longer half-lives than mRNA that are bounded at the upper limit by the cell division time, which is typically 35-60 minutes for cultured *E. coli*. Finally, the burst size, or the number of proteins synthesized for a given mRNA, has been estimated to be

between 5-40 providing limits for the translational efficiencies of the RBSs[6]. The initial values used in the simulation of our model are given in Table S3.

After obtaining initial parameters for our model, we used bifurcation analysis to determine the impact of altering a select number of the parameters. The selection of the parameters was based on the effects that the parameters had on altering the behavior of the circuit and the ability to tune these parameters experimentally. For this reason we chose to focus on the degradation rate of LuxR (k_{dR}), the rate of translation of LacI (k_{tI}), and the binding of LacI to $P_{luxI\text{-}lacO}$ (k_{IP}). As shown in Figure S5a, relaxation based oscillations only occur for degradation rates of LuxR that are ~4-10-fold faster than that of LacI. This range is expanded for systems in which the binding of LacI to the hybrid promoter is more closely balanced to the binding strength of LuxR as shown by the expanding oscillatory regime in Figure S5b for decreasing rates of LacI binding (k_{IPmax}). Finally, decreasing the rate of LacI translation relative to LuxR translation further expands the expected oscillatory regime of the circuit (Figure S5c).

Table S3. Initial parameter values used in model.

Parameter	Value	Rationale
k_{2I}	$2.4\text{x}10^{-4}$ $nM^{-1}s^{-1}$	
k_{-2I}	$2.4\text{x}10^{-2}$ s^{-1}	With k_{2I}, K_{diss} = 100 nM
k_{4I}	$4.8\text{x}10^{-2}$ $nM^{-1}s^{-1}$	
k_{-4I}	$2.4\text{x}10^{-2}$ s^{-1}	With k_{4I}, K_{diss} = 0.5 nM
k_{IPmax}	0.12 $nM^{-1}s^{-1}$	
k_{-IP}	$4\text{x}10^{-3}$ s^{-1}	With k_{IPmax}, K_{diss} = 0.03 nM
k_A	$2.5\text{x}10^{-3}$ $nM^{-1}s^{-1}$	
k_{-A}	$4.8\text{x}10^{-2}$ s^{-1}	With k_A, K_{diss} = 20 nM
k_{2A}	$2.4\text{x}10^{-4}$ $nM^{-1}s^{-1}$	
k_{-2A}	$2.4\text{x}10^{-2}$ s^{-1}	With k_{2A}, K_{diss} = 100 nM
k_{AP}	$4.8\text{x}10^{-3}$ $nM^{-1}s^{-1}$	
k_{-AP}	$4.0\text{x}10^{-3}$ s^{-1}	With k_{AP}, K_{diss} = 0.83 nM
k_{tm}	$2\text{x}10^{-5}$ s^{-1}	Adjusted
k_{tmA}	$5\text{x}10^{-3}$ s^{-1}	Adjusted
k_{tR}, k_{tI}, k_{tG}	0.1 s^{-1}	With k_{dm} gives burst rate of ~20
k_{dM}	$6\text{x}10^{-3}$ s^{-1}	Half-life of ~2 minutes
$k_{dR,}$ k_{dI}, k_{dG}	$2.57\text{x}10^{-4}$ s^{-1}	Half-life of 45 minutes
$P_{luxI\text{-}lacO}$	83 nM	Assume 50 copies/cell

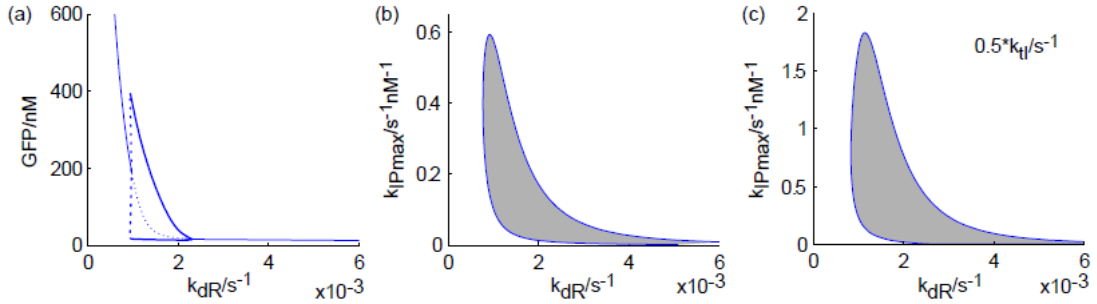

Figure S5. Bifurcation analysis of coupled feedback loop model. (a) Single parameter bifurcation diagram for the LuxR degradation rate. Stable states are shown as solid lines and unstable states are shown as dashed lines. For the oscillatory regimes, the maximum/minimum amplitudes are plotted. (b) Two-parameter bifurcation diagram for the LacI binding rate and the LuxR degradation rate. Oscillatory states are shown in gray. (c) Two-parameter bifurcation diagram as in (b) but with the LacI translation rate halved.

References

1. **M. D. Barkley and S. Bourgeois, in *The Operon*, eds. J. H. Miller and W. S. Reznikoff, Cold Spring Harbor Laboratory Press, Cold Spring Harbor, 1980, pp. 177-220.**
2. **Y. M. Wang, J. O. Tegenfeldt, W. Reisner, R. Riehn, X. J. Guan, L. Guo, I. Golding, E. C. Cox, J. Sturm and R. H. Austin, *Proc. Natl. Acad. Sci. U. S. A.*, 2005, 102, 9796-9801.**
3. **A. L. Urbanowski, C. P. Lostroh and E. P. Greenberg, *J. Bacteriol.*, 2004, 186, 631-637.**
4. **N. Qin, S. M. Callahan, P. V. Dunlap and A. M. Stevens, *J. Bacteriol.*, 2007, 189, 4127-4134.**
5. **R. Rauhut and G. Klug, *FEMS Microbiol. Rev.*, 1999, 23, 353-370.**
6. **D. Kennell and H. Riezman, *J. Mol. Biol.*, 1977, 114, 1-21.**